Electronic Supplementary Material (ESI) for Journal of Materials Chemistry A.

Electronic Supplementary Information

In situ growth of Pt_3Ni nanoparticles on A-site deficient perovskite with enhanced activity for oxygen reduction reaction

Yang Gao,[a] Jian Wang,[a] Yu-Qi Lyu,[a] Kwunyu Lam,[a] and Francesco Ciucci[a,b]*

[a] Department of Mechanical and Aerospace Engineering, The Hong Kong University of Science and Technology, Hong Kong, SAR China.

[b] Department of Chemical and Biomolecular Engineering, The Hong Kong University of Science and Technology, Hong Kong, SAR China

Methods

Materials Synthesis and Basic Characterization

$LaMnO_3$ (LMO), $La_{0.9}Mn_{0.9}Pt_{0.1}O_{3-\delta}$ (LMP), $La_{0.9}Mn_{0.9}Pt_{0.075}Ni_{0.025}O_{3-\delta}$ (LMPN), and $La_{0.8}Mn_{0.8}Pt_{0.15}Ni_{0.05}O_{3-\delta}$ (LMPN2) were synthesized via a standard sol-gel method. Stoichiometric amounts of $La(NO_3)_3 \cdot 6H_2O$, $Mn(NO_3)_2 \cdot 4H_2O$, $Pt(NH_3)_2(NO_3)_2$, and $Ni(NO_3)_2 \cdot 6H_2O$ (all analytical grade, Sigma-Aldrich) were dissolved in DI water with continuous magnetic stirring at 80 ^{o}C. Ethylene diamine tetraacetic acid (EDTA) and citric acid (CA) were then added to the solution with the mole ratio of metal atoms: EDTA: CA as 1: 1: 2. The pH of the solution was adjusted to ~6 by adding $NH_3 \cdot H_2O$. The solutions were then continuously heated to form a gel, and further heated in the oven at 250 °C to form powder precursors. The precursors were all calcined in air at 900 °C for 5 hours to form LMO, LMP, LMPN, and LMPN2, respectively. The above perovskites were then reduced in H_2 at 500 °C for 30 min for exsolution, forming the reduced form namely rLMO, Pt/rLMP, Pt_3Ni/rLMP, Pt_3Ni/rLMPN2, respectively. Pure Pt_3Ni was also synthesized following a similar method starting with $Pt(NH_3)_2(NO_3)_2$ and $Ni(NO_3)_2 \cdot 6H_2O$ and reduction in H_2.

The crystal structures of the as-prepared materials were studied with powder X-ray diffraction (XRD) using an Xpert Pro, PANalytical with a Cu Kα radiation (λ =1.5406 Å). The surface morphology and exsolved nanoparticles were examined by transmission electron microscopy (TEM, JEM-2010F) and scanning electron microscopy (SEM, JOEL-6700F). The surface valence state of Mn was examined using XPS (PHI 5600) with monochromatic Al Kα X-ray (1486.6 eV), and the bulk is characterized with a standard iodometric titration using HCl solution, KI, $Na_2S_2O_3$, and starch. The Brunauer–Emmett–Teller (BET) specific surface area was tested with a surface area and pore size analyzer (Beckman Coulter, SA3100).

Electrochemical Characterization

A rotating ring disk electrode device (RRDE-3A, BAS Inc.) setup and potentiostat (ALS2325E, BAS Inc.) were used to measure the linear sweeping voltammetry (LSV). A three-electrode setup was used with glassy carbon as the working electrode, Pt wire as the counter electrode, and Ag/AgCl (filled with 3.0 M NaCl) as the reference electrode. To measure the electron transfer number in ORR, the Pt ring electrode was also used where the potential offset was set at 0.4 V. The collection efficiency of the electrode was 0.424 according to the company. The catalyst ink was prepared by adding 10 mg perovskite/carbon mixture into 1.9 mL ethanol (99.5%, Sigma Aldrich) with 0.1 mL Nafion (perfluorinated resin solution, 5 wt.%, Sigma Aldrich). The solution was then treated in an ultrasonic bath for 30 min. 10 μL of the dispersed solution was loaded to the polished glassy carbon electrode, making the mass loading ~0.05 mg. The diameter of the electrode was 0.4 cm, therefore the surface-specific loading can be calculated to be ~0.4 mg cm^{-2}. A commercial Pt/C catalyst (20 wt.% load, Sigma Aldrich) was also tested for comparison with the same loading. The potential was converted to a reversible hydrogen electrode (RHE). 0.1 mol L^{-1} KOH solution was used as the electrolyte. The scan rate was set at 5 mV s^{-1}.

Pt mass ratio and mass activity

We calculated the mass ratio of Pt in LMPN and LMP directly from the stoichiometric material, e.g., for LMPN and Pt_3Ni/LMPN, we used $La_{0.9}Mn_{0.9}Ni_{0.025}Pt_{0.075}O_3$ and computed Pt mass ratio to be:

$m_{Pt} \approx 0.075M_{Pt} / (0.9M_{La} + 0.9M_{Mn} + 0.025M_{Ni} + 0.075M_{Pt} + 3M_O) \approx 0.06$,

where M is the molar mass of each element. For LMPN2 and Pt_3Ni/LMPN2, a similar calculation gives $m_{Pt} \approx 0.12$.

For the actual catalyst, the Pt mass ratio is further reduced by adding carbon. For example, for Pt_3Ni/rLMPN/VC mixtures with the mass ratios of 1:3, 1:1, and 3:1, the Pt mass ratios become ¼, ½, and ¾ of that in the pure Pt_3Ni/rLMPN, i.e., 0.015, 0.030, and 0.045, respectively.

To calculate the total mass activity and Pt mass activity, we simply divided the current density at 0.9 V by the total mass loading (0.05 mg for all materials, as calculated in the electrochemical characterization section), and the Pt mass loading (as computed above), respectively.

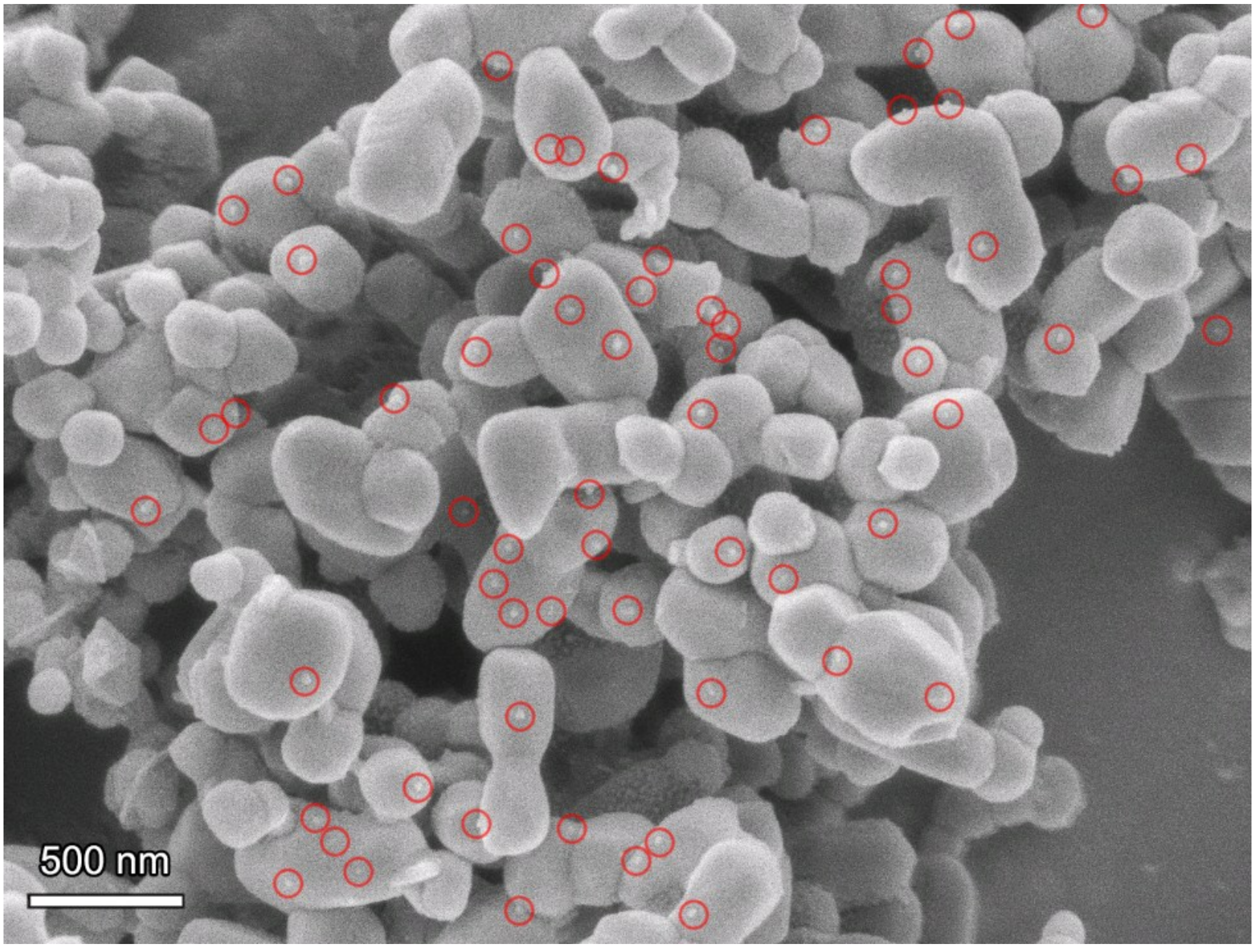

Figure S1. SEM images of Pt_3Ni/rLMPN overall morphology. Nanoparticles are highlighted by red circles.

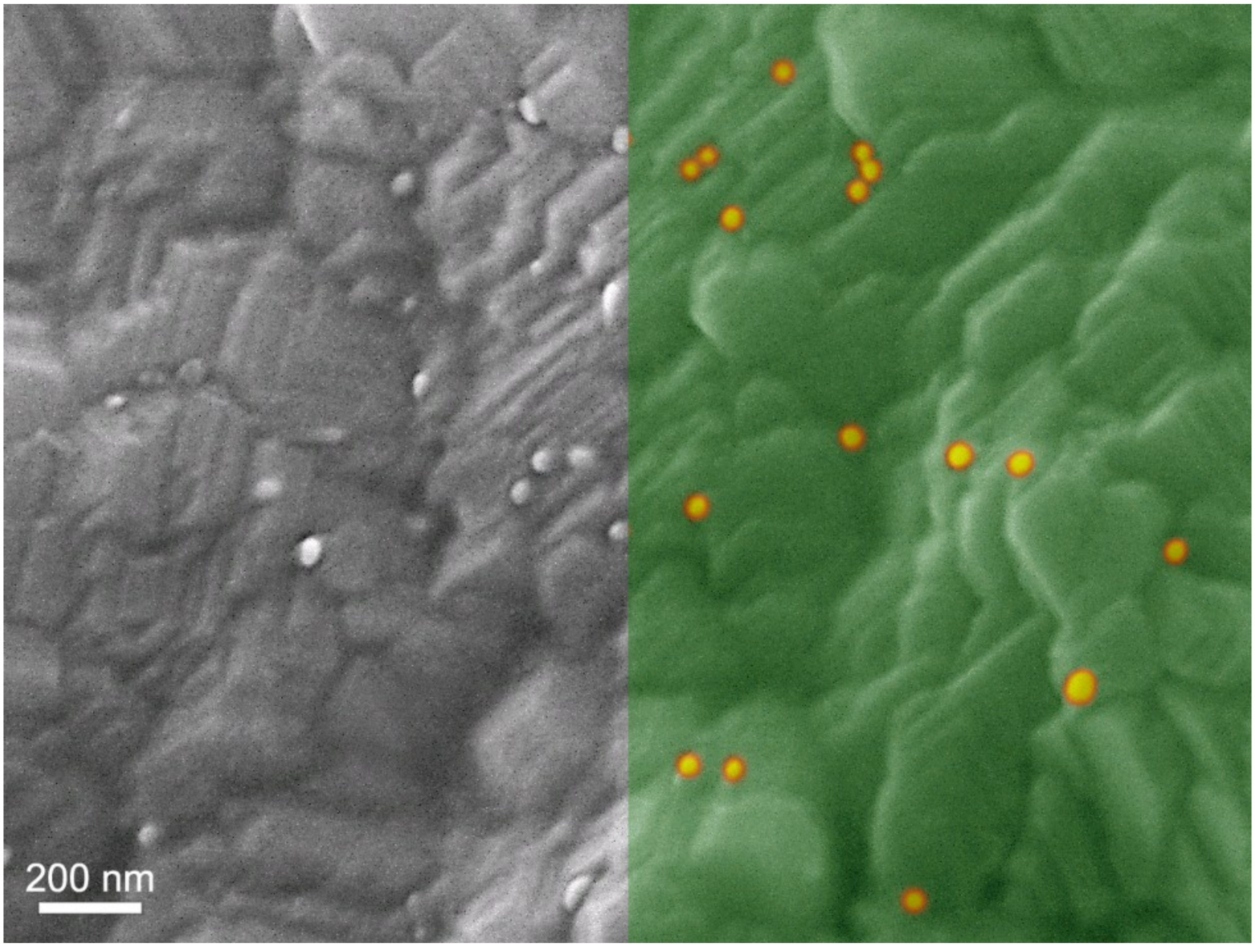

Figure S2. SEM images of Pt/rLMP. False color is used on the right side to highlight the particles.

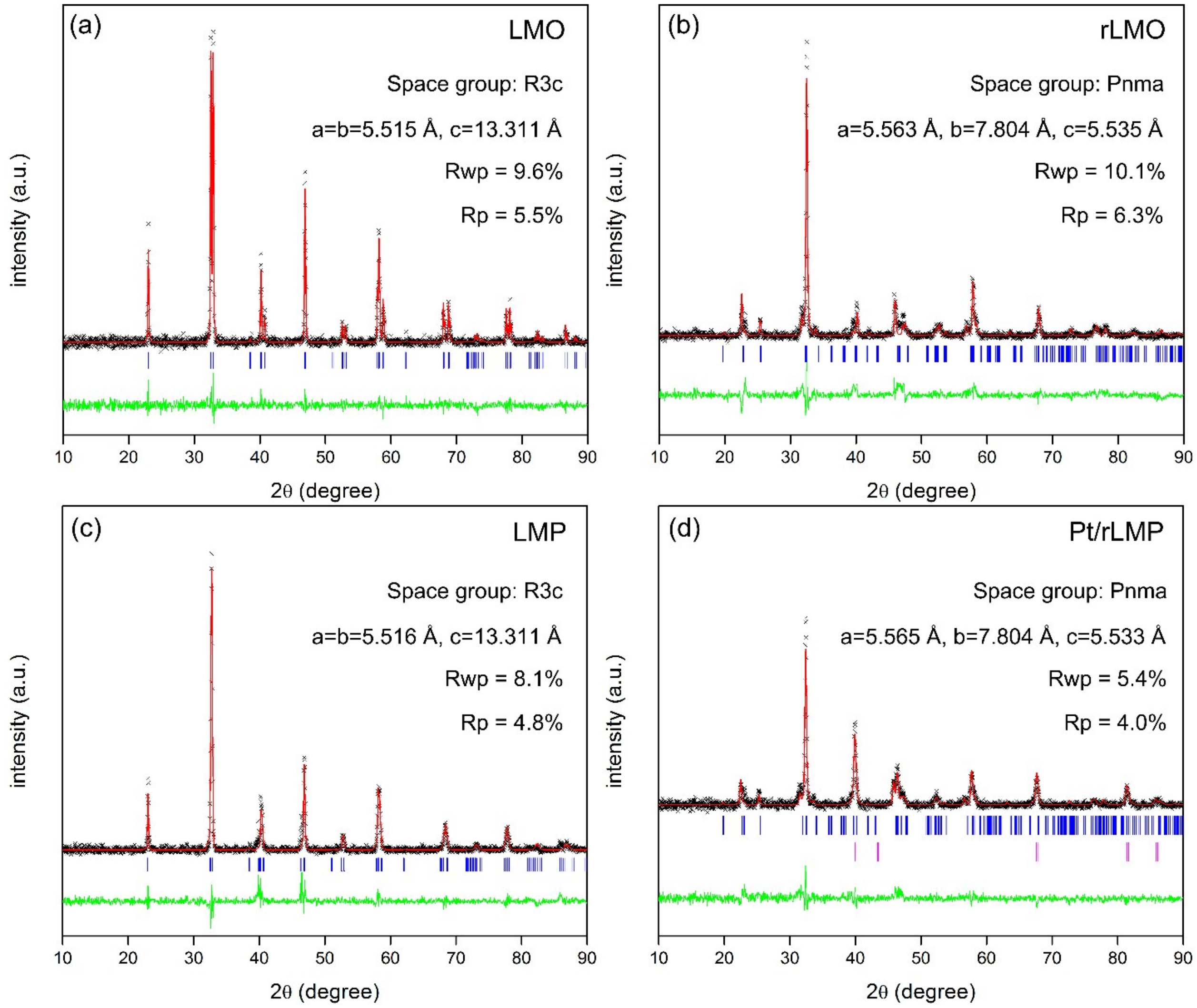

Figure S3. XRD patterns with refinement of LMO (a), rLMO (b), LMP (c), and Pt/rLMP (d). The x marks indicate the experimental data, red lines are calculated patterns, and green lines are the residuals. The vertical bars indicate the peaks of the refined perovskite (blue) and Pt metal (magenta) crystal structures.

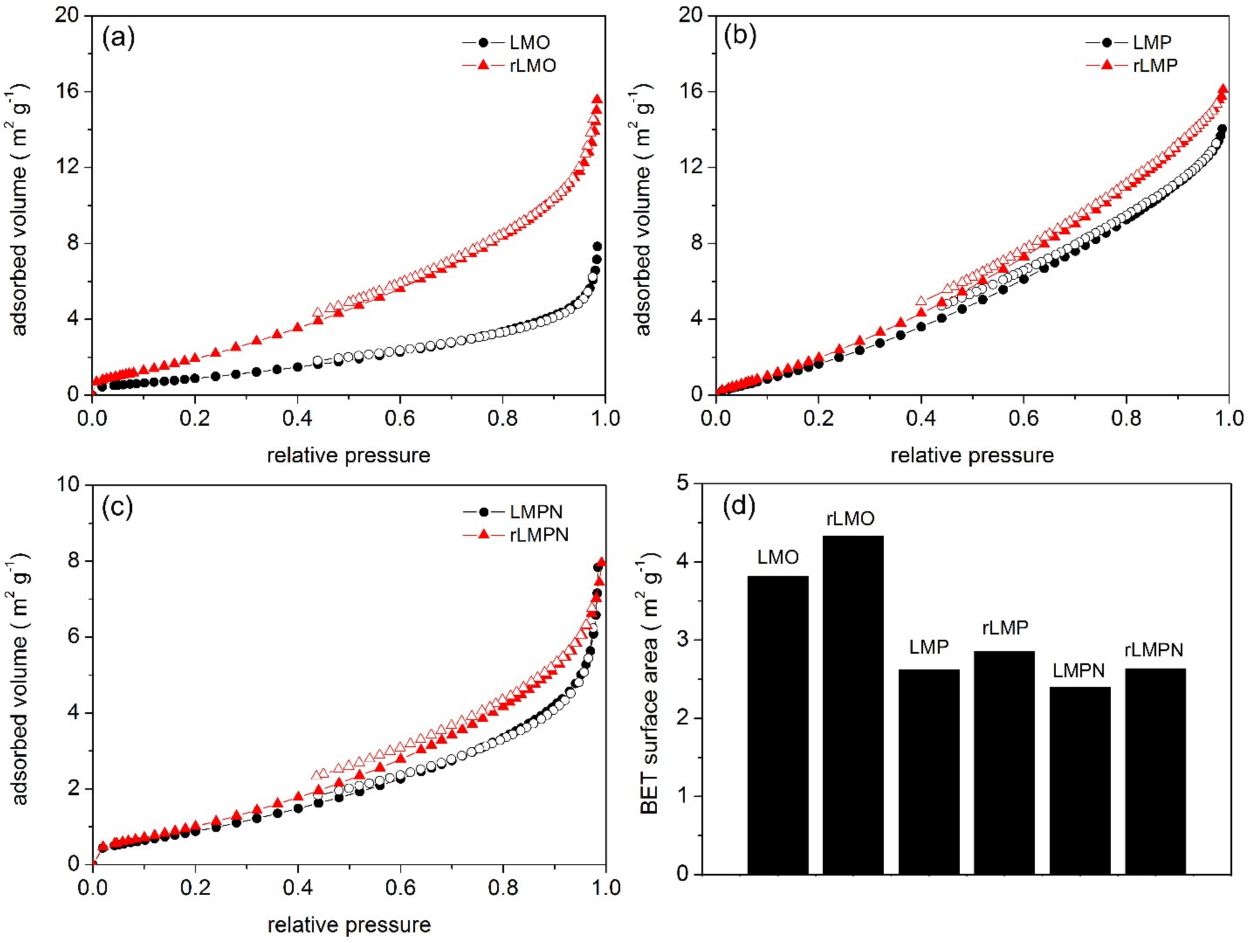

Figure S4. (a, b, c) Nitrogen adsorption/desorption isotherm curves of LMO, LMP, LMPN, and their reduced form. (d) Brunauer–Emmett–Teller specific surface area of the above samples.

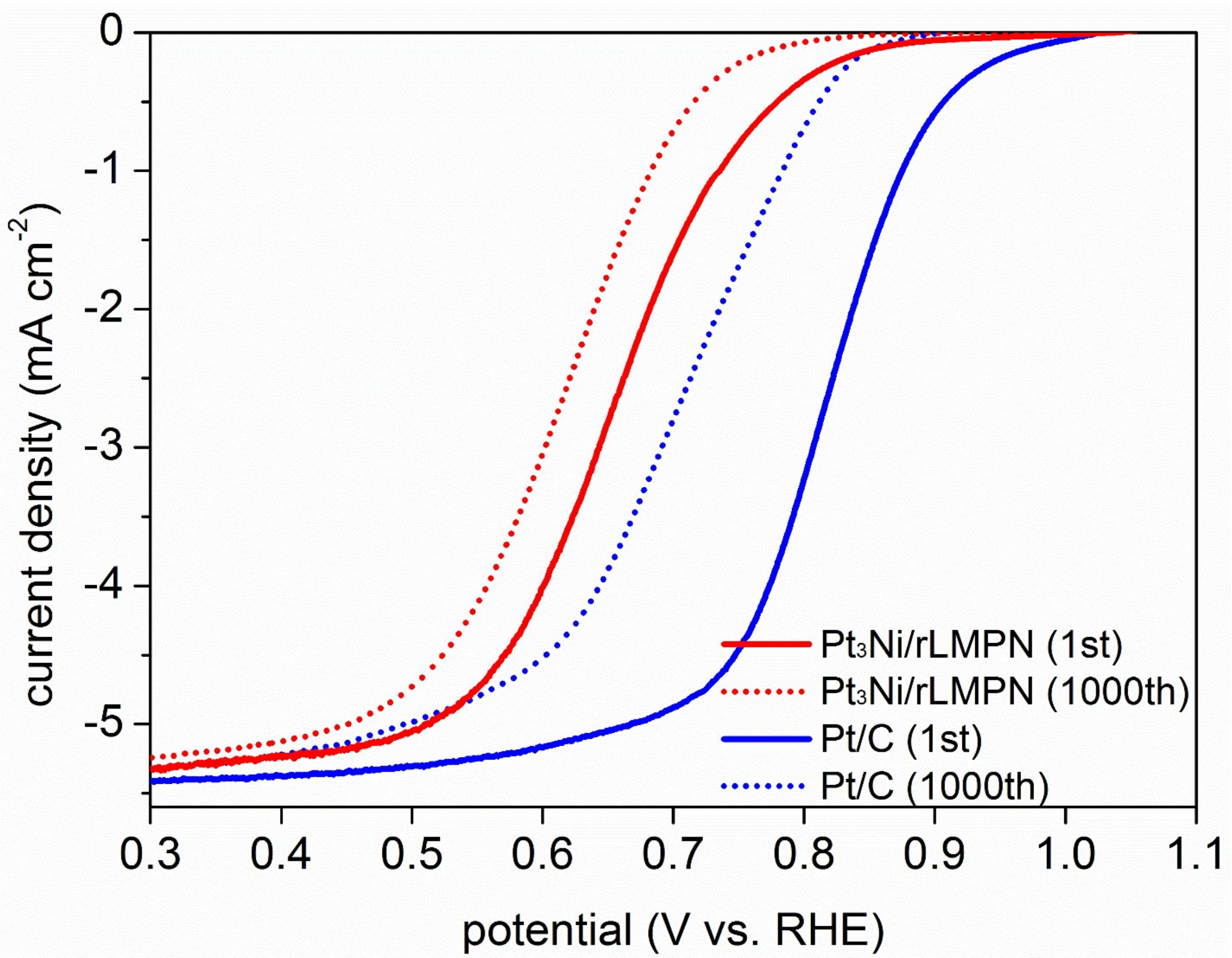

Figure S5. ORR activity of Pt_3Ni/rLMPN and Pt/C before and after 1000 cycles.

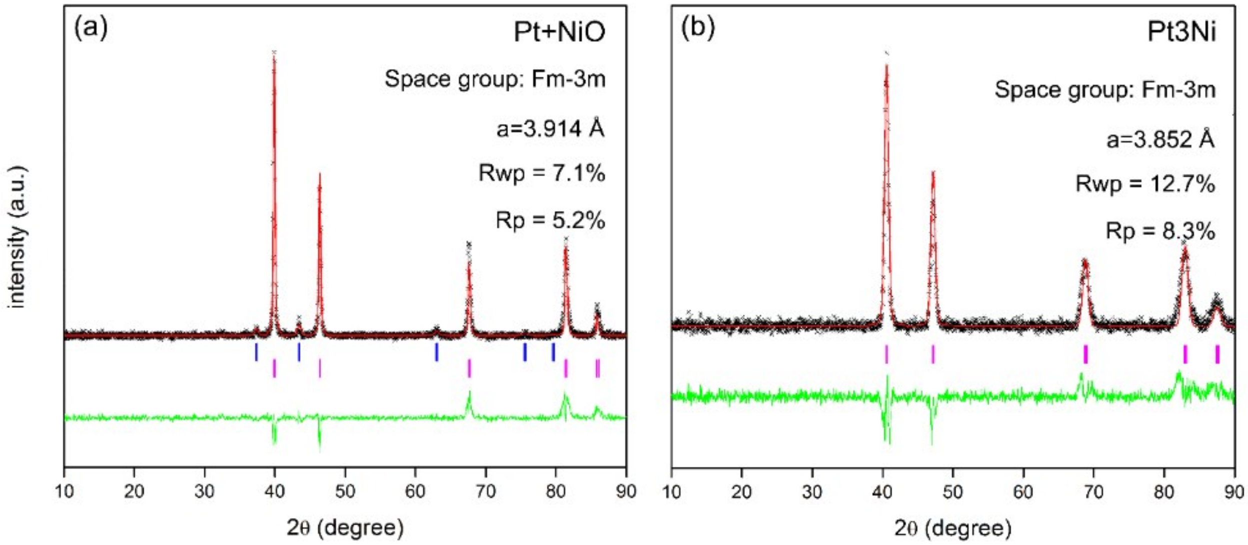

Figure S6. (a) XRD pattern of Pt_3Ni sample before reduction. The material is composed of 74% Pt phase (magenta) and 26% NiO phase (blue). (b) XRD pattern of Pt_3Ni sample after reduction. The material is composed of pure Pt_3Ni phase (magenta). The lattice parameter decreases after the formation of Pt_3Ni. The particle size can be estimated using the Scherrer equation as ~40 nm.

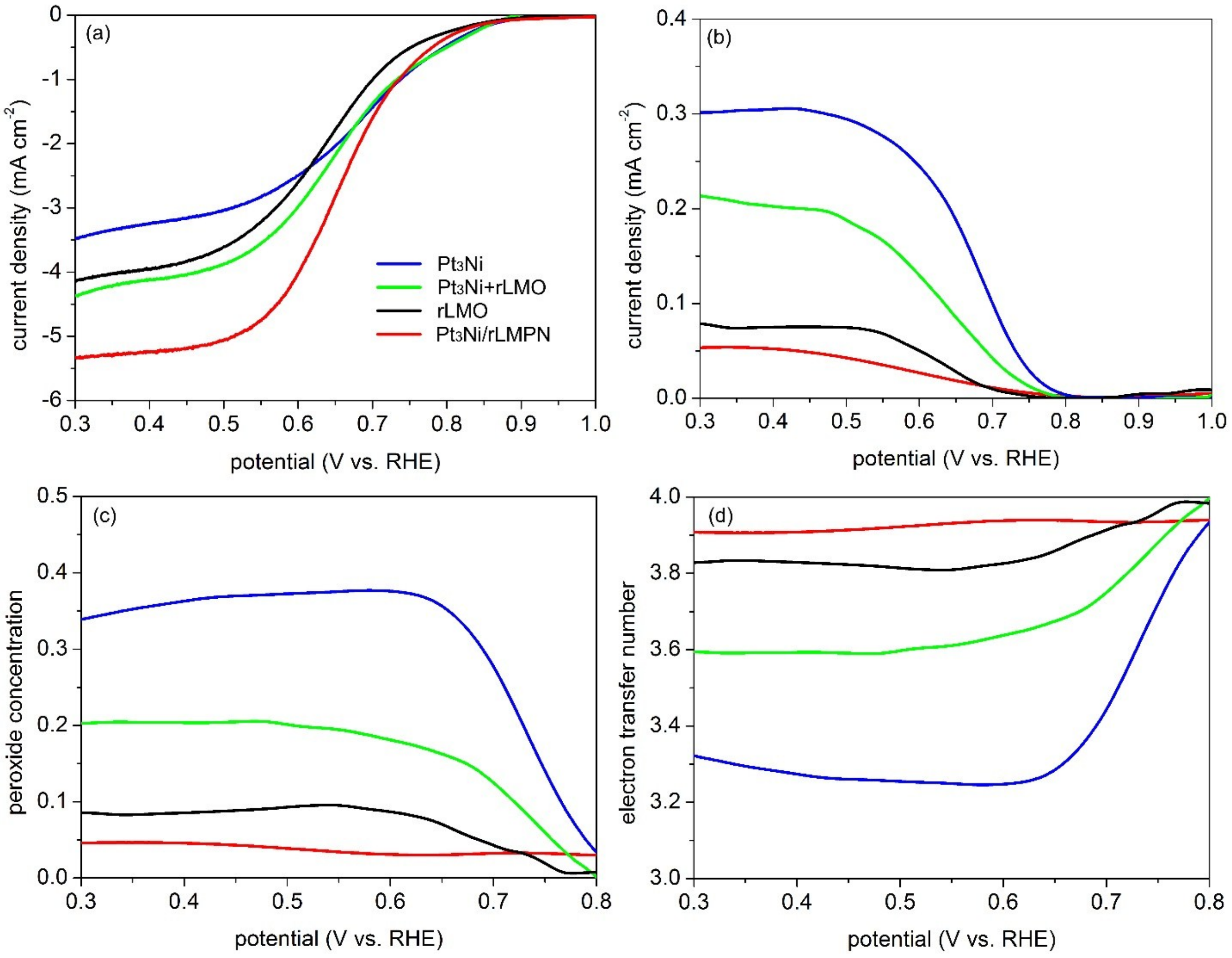

Figure S7. (a) ORR activity of 10% Pt_3Ni mixed with 90% VC carbon, 5% Pt_3Ni mixed with 78% rLMO and 17% carbon, 83% rLMO mixed with 17% carbon, and 83% Pt_3Ni/rLMPN mixed with 17% carbon, respectively. (b) corresponding ring current density, (c) peroxide ratio, (d) and electron transfer number. The same color scheme of panel (a) is used in all the four panels.

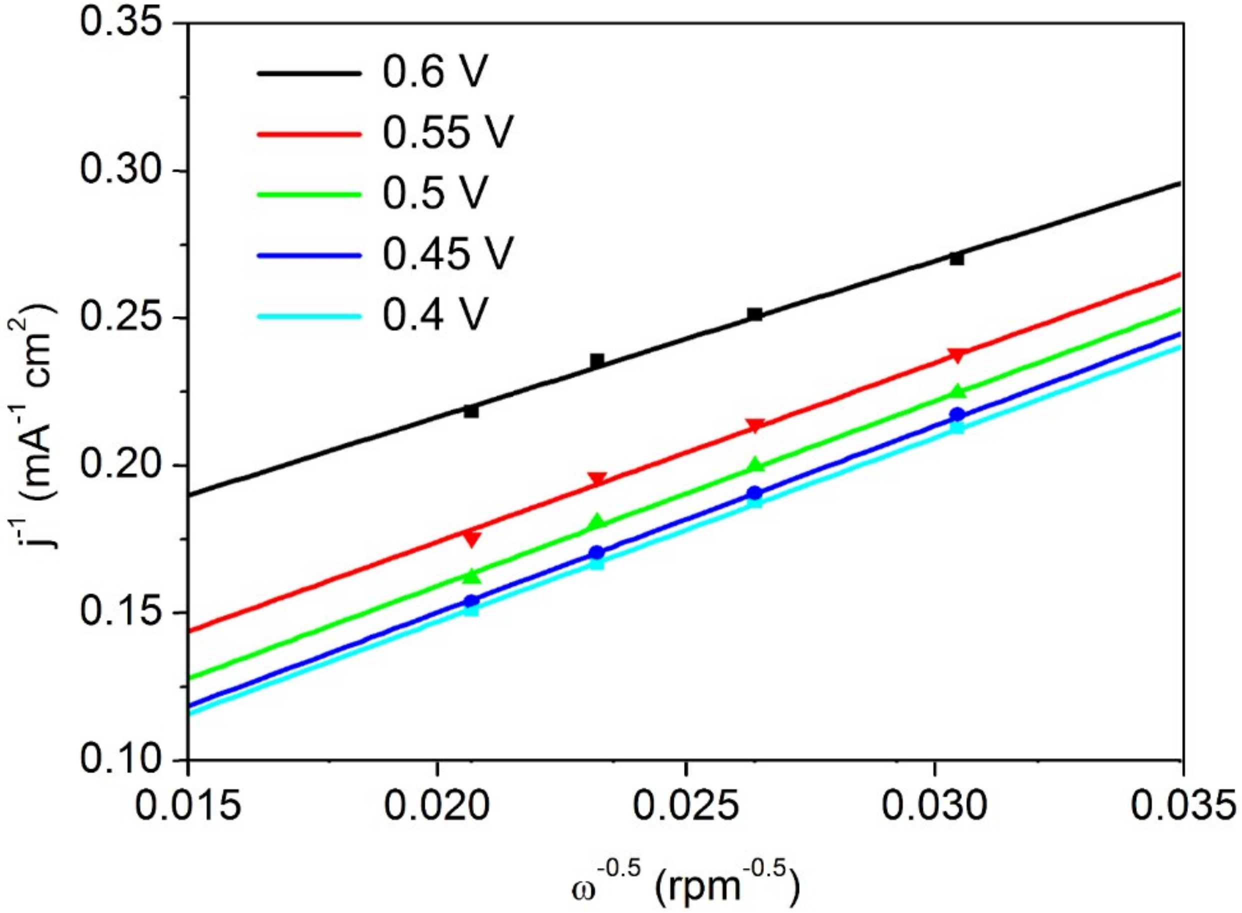

Figure S8. The corresponding Koutecky–Levich plot of Pt_3Ni/rLMPN in Figure 4a.

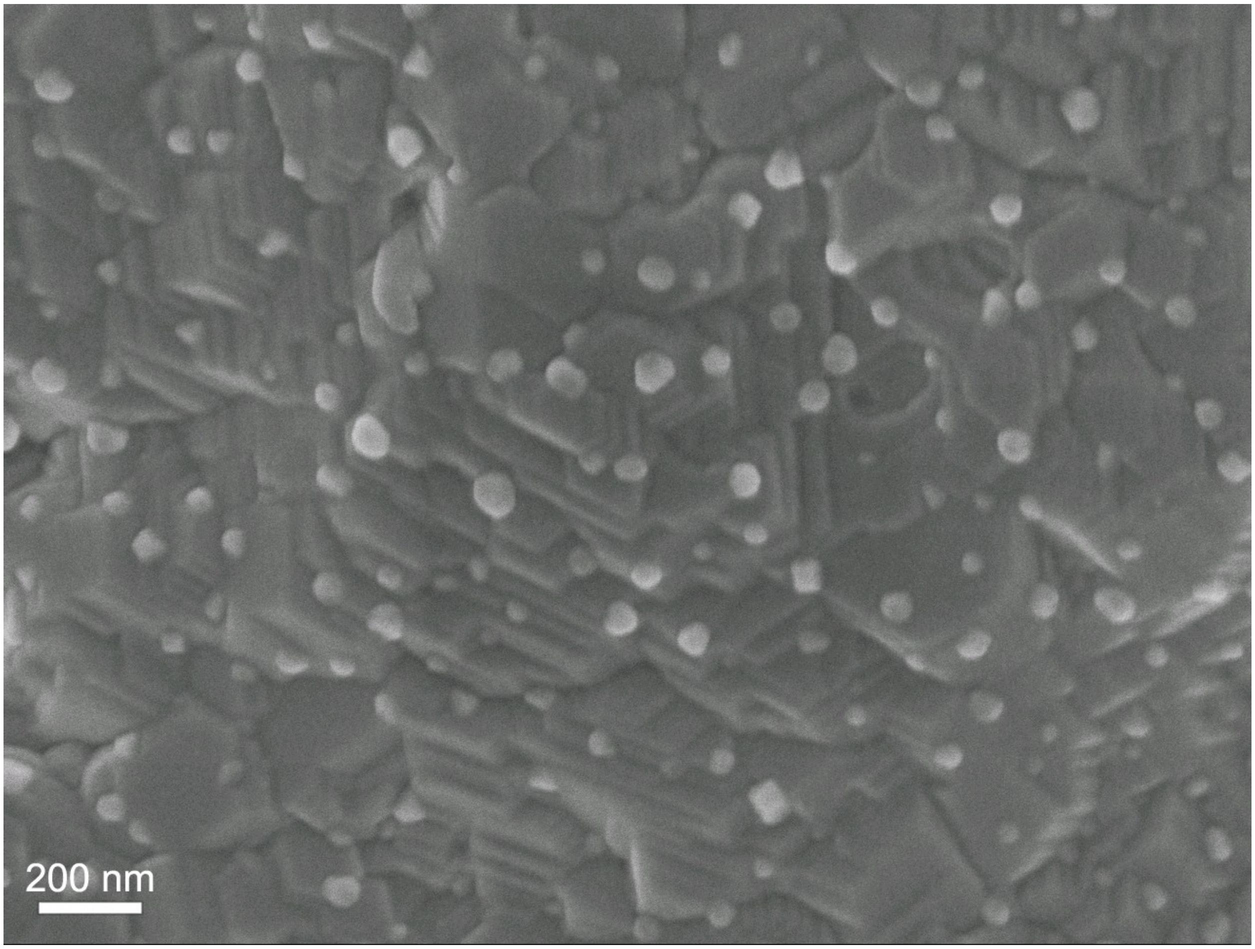

Figure S9. SEM image of Pt_3Ni/rLMPN2.

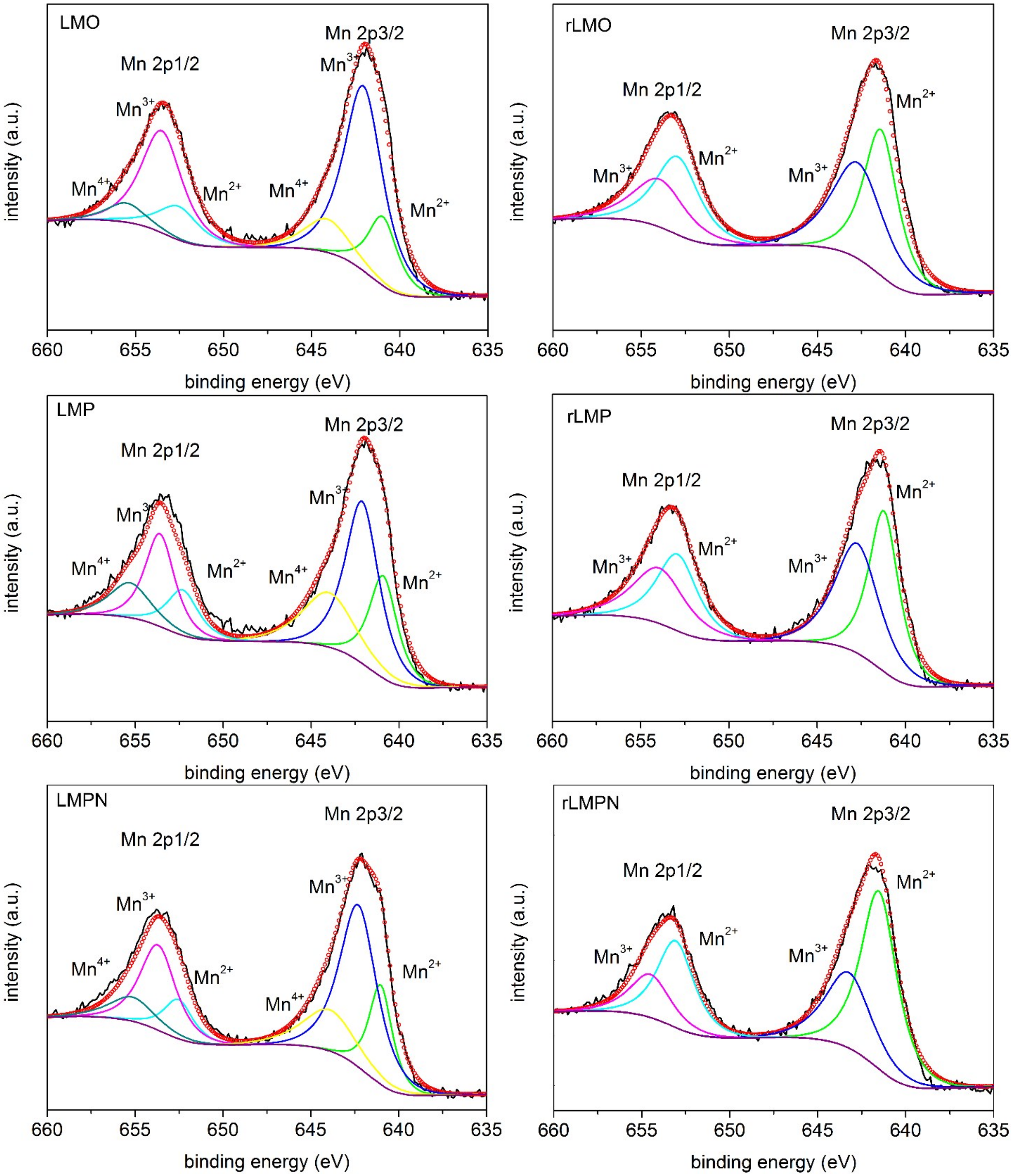

Figure S10. XPS spectra of Mn 2p with the deconvolution of the peaks for all the perovskite materials.

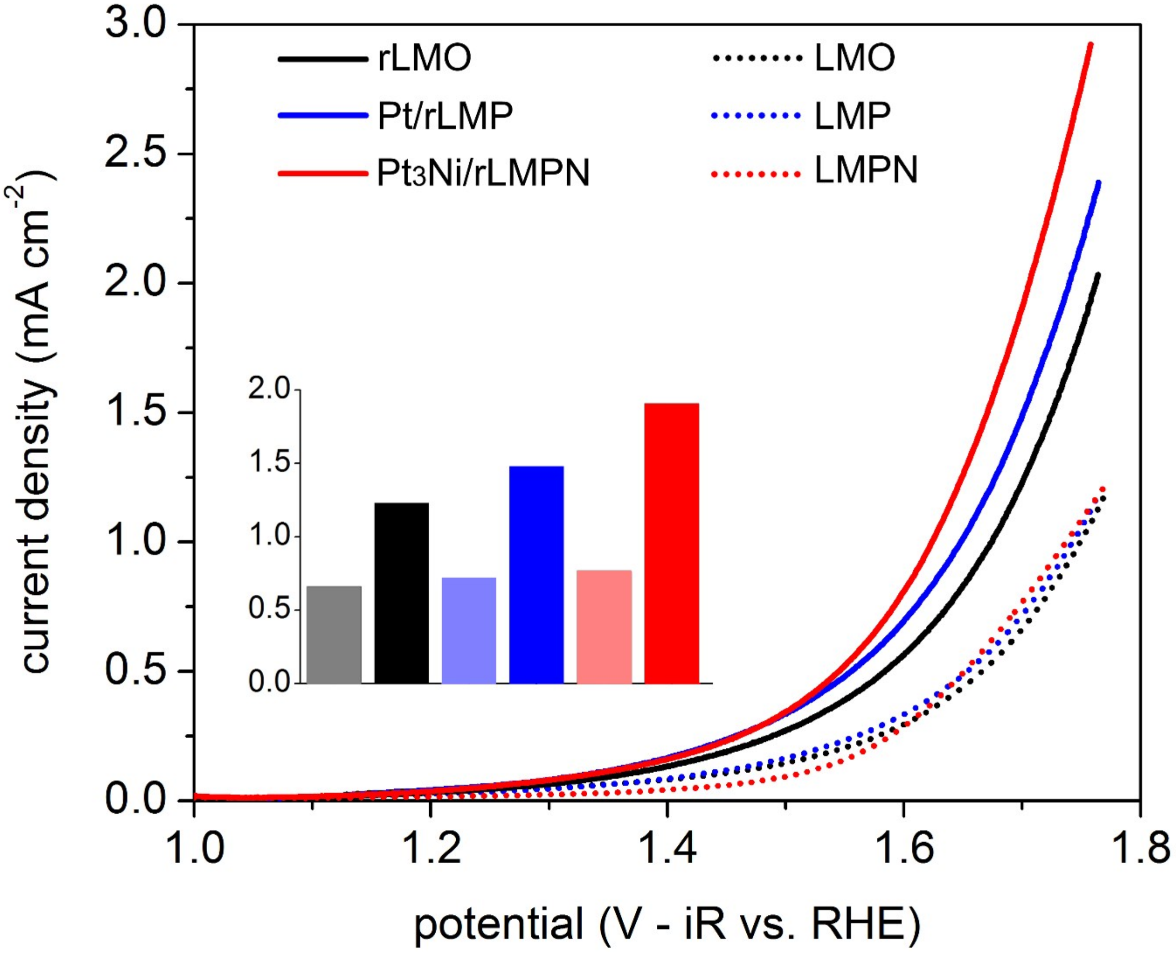

Figure S11. OER current densities of LMO, rLMO, LMP, Pt/rLMP, LMPN, and Pt_3Ni/rLMPN at 1600 rpm in O_2 saturated 0.1 mol L^{-1} KOH solution with a scan rate of 5 mV s^{-1}. The inset shows the current density at 1.7 V.

Table S1. Atomic concentration of each element as obtained from XPS. The stoichiometry ratio is calculated from $La_{0.9}Mn_{0.9}Pt_{0.075}Ni_{0.025}O_3$.

	LMPN	rLMPN	Stoichiometry
La	0.2015	0.2025	0.2
Mn	0.1624	0.1442	0.18
Pt	0.0051	0.0105	0.015
Ni	0.0012	0.0036	0.005
O	0.6297	0.6393	0.6

Table S2. Comparison of the ORR activity of some common perovskite catalysts.

	Onset potential (V vs RHE)	Tafel Slope (mV dec^{-1})	Reference (main text)
Pt_3Ni/rLMPN	0.92	76	This work
$LaMnO_3$	0.77	147	This work
$(PrBa_{0.8}Ca_{0.2})_{0.95}(Co_{1.5}Fe_{0.5})_{0\cdot 95}Co_{0.05}O_{5+\delta}$	0.95	40	[16]
RO-$LaFe_{0.95}Pd_{0.05}O_3$	0.80	78	[17]
H-Pt/$CaMnO_3$	0.90	65, 109 (two	[18]
$La_{0.3}(Ba_{0.5}Sr_{0.5})_{0.7}Co_{0.8}Fe_{0.2}O_{3-\delta}$	0.78	/	[19]
$LaCoO_3$	0.80	/	[29]
$LaFeO_3$	0.70	/	[29]
$LaMnO_{3+\delta}$	0.90	162	[30]
$LaNiO_{3-\delta}$	0.85	103	[31]
$La_{(1-x)}Sr_xMnO_3$	0.88	/	[32]
$La_{0.95}FeO_{3-\delta}$	0.70	/	[33]
$NdBa_{0.75}Ca_{0.25}Co_{1.5}Fe_{0.5}O_{5+\delta}$	0.85	/	[34]

Table S3. Valence states of Mn obtained from XPS and titration.

	XPS	Iodometric titration
LMO	2.98	3.14
rLMO	2.59	2.72
LMP	3.00	3.11
rLMP	2.52	2.75
LMPN	3.05	3.09
rLMPN	2.41	2.71